Energy Equip. Sys./ Vol. 12/No. 3/September 2024/ 185-196

ENERGY EQUIPSYS

Energy Equipment and Systems

www.energyequipsys.com

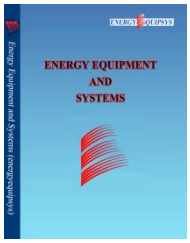

Numerical investigation of turbulent jet array impinging on smooth curved leading edge channel of gas turbine blade

Manuscript Type

Research Paper

Authors

Hooman Bahman Jahromi[a*]
Farshad Kowsary [a]

[a] School of Mechanical Engineering, College of Engineering, University of Tehran, Tehran, Iran

Article history:

Received : 12 April 2024
Accepted : 15 May 2024

ABSTRACT

Turbulent impinging jet array is one of the most efficient and popular techniques for cooling gas turbine blades. In the present paper, we numerically investigated how the geometrical design parameters affect the cooling performance for jet array impinged to a curved target. The influence parameters, including jet spacing ($2.5 \leq P_j \leq 10$), jet angle ($-45° \leq \theta \leq 45°$), and off-center distance ($0 \leq E_j \leq 6$) on average Nusselt number ($\overline{Nu}$), air pressure drop (Δp), and heat transfer uniformity index (UI) were identified through a parametric study at a constant total mass flow rate. Results show, increasing jet spacing improved heat transfer but lowered uniformity and required more compression power. Tilting the jets generally decreases the average Nusselt number but boosts the uniformity. Also, increasing the inclination angle reduces the pressure drop. Moving the jets off-center consistently lowered pressure drop until $E_j = 4$ and average Nusselt number till $E_j = 2$ without affecting uniformity much up to until $E_j = 3$, and beyond those values, increased them. best performance based on average Nusselt number is achieved for the case of $P_j = 10$, $\theta = 0$, and $E_j = 0$. Also, the uniformity index is maximized and pressure drop is minimized at $P_j = 5$, $\theta = 45°$, and $E_j = 0$.

Keywords: Impinging Jet Array, Curved Target, Leading Edge Cooling, Computational Fluid Dynamics (CFD).

1. Introduction

Impingement of jet array finds extensive use in numerous industrial applications, notably in the internal cooling of gas turbine blades [1,2].With the continuously increasing demand for energy, there is a pressing need to design more effective blade cooling technologies. Recent studies often utilize jet array impingement over flat surfaces to simulate the sides of the blade [3,4], or on curved targets to model leading edge of blade [5,6], as depicted in Fig. 1. The former was investigated in our previous work [7]. This study primarily concentrates on the latter application.

The studies about impinging jets on curved surfaces were first conducted for single jets. Using CFD, Taghinia et al. [8] investigated the impinging jet's heat transfer and flow field characteristics on a curved surface.

* Corresponding author: Hooman Bahman Jahromi
School of Mechanical Engineering, College of Engineering, University of Tehran, Tehran, Iran
E-mail address: Hooman.Bahman@ut.ac.ir

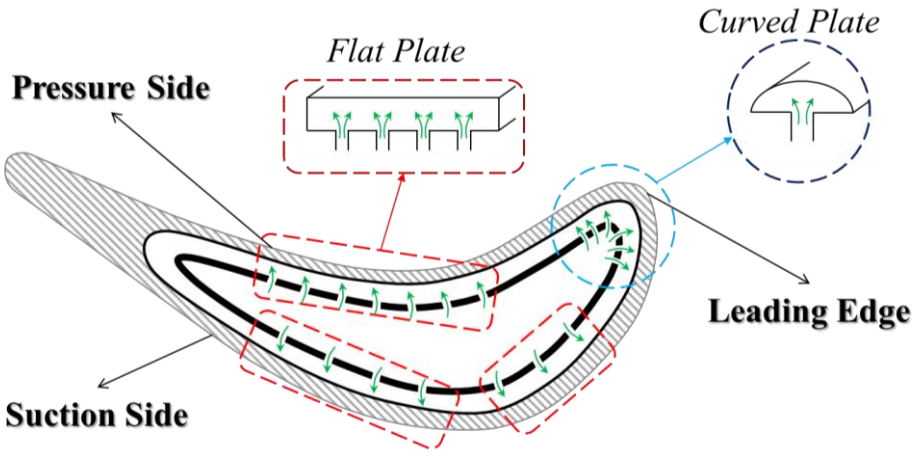

Fig. 1. Impingement cooling of gas turbine blade sides and leading edge [7].

Three turbulence models are compared with experimental data, including RNG k-ε, the one-equation model (OEM), and the SST-SAS model. The results show that the one-equation model and SST-SAS model provide better agreement with the experimental data for the local Nusselt number distribution. The study highlights the influence of the jet height on the accuracy of predictions, with the OEM model performing better at lower heights. Additionally, the paper details the methodology of the SST-SAS model, which is a combination of RANS and LES models, and discusses the limitations and advantages of the different turbulence models. Zhou et al. [9] presented an experimental study on the effects of surface curvature on jet impingement heat transfer. The study involved using a steel pipe with a round nozzle to create a high-pressure jet of air that impinged on various concave surfaces. The impingement curved surfaces had different diameters, and a flat surface was also included in the experiments. The study investigated surface curvature's enhancement and confinement effects on heat transfer, analyzing Nusselt number distributions and velocity profiles. The findings indicated that surface curvature had a negative impact on heat transfer, and increasing the jet height reduces the Nusselt number. Also, the study provided experimentally verified correlations for the average Nusselt number over the curved surface. Poitras et al. [10] studied the aerodynamic and heat transfer analysis of an impinging jet on a concave surface through numerical simulations and experimental validations. The study focuses on the oscillatory behavior of the jet inside the cavity for different geometric configurations. The results show that the jet oscillates within the cavity for specific Reynolds numbers and geometries, leading to a uniform pressure and heat transfer distribution on the concave surface. The frequency of oscillation is influenced by the geometry of the cavity, with higher impact heights resulting in lower frequencies.

The jet array impingement studies were noticed later. The research paper by Yang et al. [11] investigates heat transfer in an array of impinging jets on a concave surface through a combination of numerical simulations and experimental studies. The experiments were conducted, focusing on the heat transfer characteristics of impinging jets on the leading edge of a wing using the NACA0015 airfoil. The study explores the effects of different turbulence models on multi-jet impingement computation and the influence of the jet diameter (D) and spacing (p), impingement height (h), and inclination angle (θ) on heat transfer characteristics. Important findings include the potential enhancement of heat transfer capacity with specific structure variables ($h/D = 10$, $p/D = 6$, and $\theta = 15°$) and the limited improvement in heat transfer performance by enlarging jet hole diameters in aircraft anti-icing systems. The paper by Wu et al. [12] investigates leading edge impingement cooling of a turbine blade. The study validates a numerical strategy using the RNG k-ε

turbulence model and compares impingement cooling models with and without separators. The findings indicate that matching jet Reynolds number, mass flow ratio, and temperature ratio to real conditions is crucial for accurate predictions of Nusselt numbers. The use of separators in impingement cooling hinders heat transfer attenuation caused by the crossflow effect, significantly improving cooling effectiveness. New correlations between surface averaged Nusselt number, jet Reynolds number, and temperature ratio are suggested for gas turbine operating conditions.

The effects of elongated jet holes on staggered array jet impingement cooling on a semi-circular concave surface was numerically studied by Ümit Tepe [13], focusing on heat transfer and flow characteristics for potential turbine blade cooling applications. The study compares the performance of elongated jet holes with normal staggered array jet impingement using CFD simulations with different jet Reynolds numbers, plate distances, and jet-to-plate gaps. The results show that decreasing the jet-to-plate gap leads to increased heat transfer, with up to a 20.16% enhancement achieved at specific conditions. The study also evaluates the Thermal Performance Factor (TPF) and pressure drop, concluding that elongated jet holes can be a feasible heat transfer enhancement design for staggered array jet impingement on a concave surface despite potential manufacturing challenges for practical applications. Through numerical simulations, Qiu et al. [14] investigated the flow structure and heat transfer characteristics of jets impinging onto a concave surface with varying jet arrangements and Reynolds numbers. The study focuses on an array jets arrangement as the baseline and compares it with three array cases with inline and staggered patterns. The results show that the heat transfer uniformity is significantly enhanced in both inline and staggered cases compared to the array jets case. The study also reveals that the curved surface-averaged Nusselt number increases with increasing jet spacing at inline arrangement. Akgul et al. [15] investigated optimizing heat transfer and entropy generation in impinging jet cooling on a curved surface using Al2O3/water nanofluid. They studied different parameters such as nanofluid volume fractions, target distance-to-nozzle diameter ratio, and Reynolds numbers. The results showed that the distance-to-nozzle diameter ratio greatly impacted heat transfer enhancement and entropy generation improvement. The highest Nusselt number and the lowest entropy generation were achieved with blade-shaped alumina nanofluid at a distance-to-nozzle diameter ratio of 2. The study utilized Response Surface Methodology (RSM) and Grey Relational Analysis (GRA) to optimize the performance of the impinging jet cooling system, highlighting the importance of considering multiple factors in achieving optimal results.

Unlike prior research that focused on single jets impacting curved surfaces, this study breaks new ground by examining the impact of jet arrays on cooling performance. Existing literature on jet arrays primarily explores the influence of jet height, jet spacing, and Reynolds number on Nusselt number. Our work takes a more comprehensive approach. Through a numerical parametric study, we investigate how different design variables – jet spacing, inclination angle, and off-center distance – affect not only the Nusselt number but also two critical yet unexplored parameters: pressure drop and heat transfer uniformity index at a fixed mass flow rate. This more profound understanding of the interplay between these factors can significantly benefit the design of optimal cooling systems for gas turbine blade leading edges.

Nomenclature

p	Pressure (Pa)
T	Temperature (K)
u	Velocity component (m/s)
q	Heat flux (W/m^2)
h	Convection heat transfer coefficient (W/m2 K)
p	Pitch (m)
P	Dimensionless pitch
e	jet off-center distance (m)
E	Dimensionless jet off-center distance
D	diameter (m)
A	Area (m^2)

Greek Letters

θ	Jet inclination angle
ρ	Density (kg/m^3)
μ	Dynamic viscosity (Pa s)
κ	Thermal conductivity (W/m K)

Dimensionless Numbers

Re	Reynolds number
Pr	Prandtl number
Nu	Nusselt number

Subscripts

x	Streamwise direction
y	Spanwise direction
z	Normal direction
j	Jet
w	wall
ref	Reference

Abbreviations

RANS	Reynolds-averaged Navier-Stokes
CFD	Computational fluid dynamics
UI	Uniformity index

2. Methods and materials

2.1. Model configurations

This work employs air as the cooling fluid, with details of air properties displayed in Table 1. Figure 2(a) illustrates the computational domain under investigation. Cooling air enters the plenum and then flows through the array jets with diameters represented by $D = 10\,mm$, with the flow exiting impingement channel at the boundary condition of pressure outlet. In this configuration, the jets are spaced apart in the x direction by p. The target is a semi-circular surface of 80 mm diameter, resulting in a hydraulic diameter of $d_h = 48.8\,mm$ for impingement channel. The length of jet nozzles is set to 14 mm. As shown by Fig. 2(b), the inclination angle of jets with respect to the x direction is shown by θ. Also, according to Fig. 2(c), the amount of nozzle deviation from the impingement channel center is identified by off-center distance, e.

2.2. Data reduction

The simulations are performed for a constant mass flow rate of 0.0368 kg/s. Table 2 outlines the operational range of parameters.

The heat transfer results of this study are interpreted by Nusselt number, is defined as:

$$Nu = \frac{d_h}{\kappa}\frac{q}{T_w - T_{ref}}, \tag{1}$$

where, κ shows thermal conductivity of fluid and q shows heat flux. Also, T_w and T_{ref} denote the wall and reference temperature, respectively. The air pressure drop is denoted by $\Delta\mathcal{p}$.

Also, the heat transfer uniformity (UI), is calculated from [16],

$$UI = 1 - \frac{\sum_{i=1}^{n}\sqrt{(Nu_i - \overline{Nu})^2}A_i}{\overline{Nu}\sum_{i=1}^{n}A_i}, \tag{2}$$

where A_i shows the area of ith cell.

2.3. Governing equations

In this study, RANS equations are solved for the incompressible and steady-state flow:

- Continuity:

$$\nabla \cdot u = 0 \tag{3}$$

- Momentum:

$$\nabla \cdot (\rho u u) = -\nabla \mathcal{p} + \nabla \cdot [(\mu + \mu_t)\nabla u] \tag{4}$$

- Energy:

$$\nabla \cdot (\rho u T) = \nabla \cdot \left[\left(\frac{\mu}{\mathrm{Pr}} + \frac{\mu_t}{\mathrm{Pr_t}}\right)\nabla T\right] \tag{5}$$

$\mathcal{p}$ is the pressure field, T is the temperature, and u is the velocity vector. $Pr_t = 0.85$ indicated the turbulent Prandtl number. The turbulent dynamic viscosity (μ_t) calculated by the SST $k-\omega$ model.

Table 1. Thermophysical properties of air.

Density, ρ (kg/m^3)	Thermal conductivity, κ $(W/m\,K)$	Dynamic viscosity, μ $(Pa\,s)$	Prandtl number, Pr
1.225	0.0242	1.79×10^{-5}	0.744

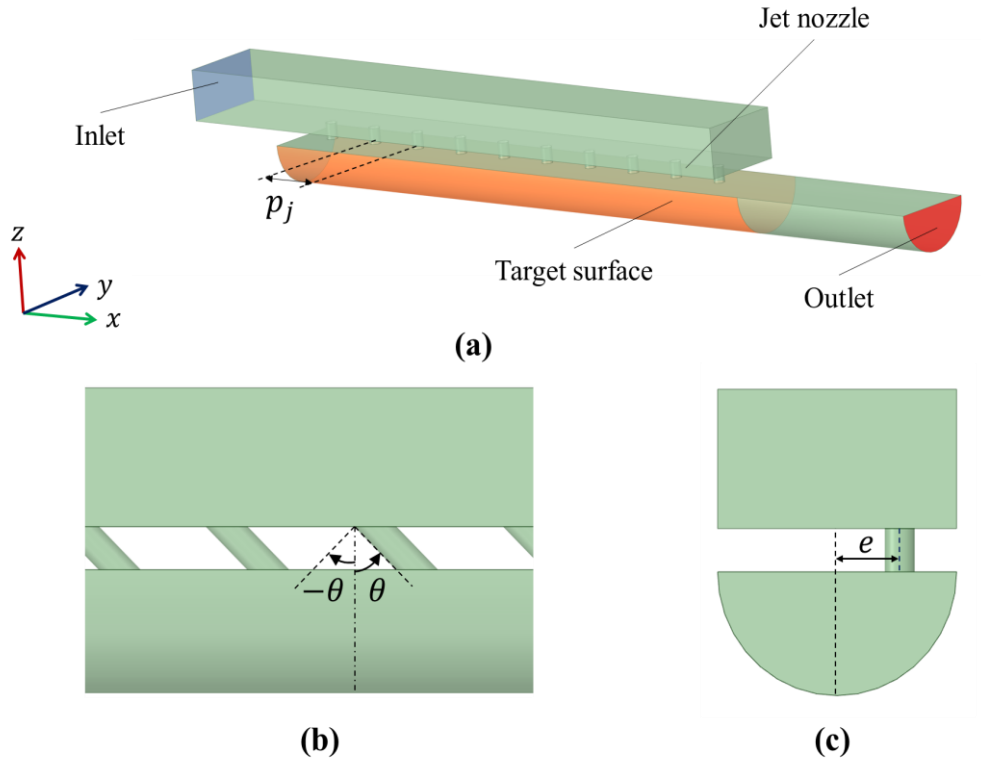

Fig. 2. (a) Schematic physical domain of jet impingement cooling. Representation of design variables: (b) jet inclination angle, and (c) jet off-center distance.

Table 2. Operating parameters in simulations.

Parameter	$P_j = p_j/D$	$E_j = e/D$	θ (°)
Range	2.5 – 10	0 – 6	–45 – +45

The governing equations undergo discretization using the finite volume method. Pressure-velocity coupling is achieved through the use of the SIMPLE algorithm. Constant mass flow rate and temperature boundary conditions are applied to inlet. The walls are assigned a no-slip boundary condition. A constant 1000 W/m^2 heat flux is exercised to the target plate. Finally, atmospheric pressure is applied for outlet.

2.4. Grid independence test

A scenario involving perpendicular jet array impingement with $P_j = 5$, $E_j = 0$, and $\theta = 0°$ is examined at constant mass flow rate. Four grid configurations are assessed: coarser, coarse, normal, and fine. The variations of average Nusselt numbers with different grid systems are presented in Table 3 for different grid systems. The normal mesh system is chosen for this research.

2.5. Simulation validation

The current study simulates a numerical dataset from Brakmann et al. [17] concerning the validation of an array of jets on a smooth target plate.

Figure 3 illustrates a comparison between the outcomes. Both numerical investigations demonstrate similar trends and values. The present study's findings align well with the results in [17].

3. Results and Discussion

This section delves into the numerical investigation of the impact of flow and geometrical variables on the heat transfer attributes

of jet arrays impinging over the curved target surface. It explores how heat transfer is reliant on flow structures. Subsequently, it thoroughly scrutinizes the design variables' impact, such as jet spacing, inclination angle, and off-center distance, on heat transfer uniformity, average Nusselt number, and air pressure drop through a parametric study.

3.1. Fluid flow

Figure 4 depicts the obtained flow streamlines and velocity contours of a perpendicular impinging jet array with no off-center distance at $P_j = 5$, $E_j = 0$, and $\theta = 0°$. Referring to Fig. 4(a), the upstream initial jet resembles a distribution field typical of single-jet impingement, displaying symmetrical radial streamlines. A crossflow emerges as the flow progresses downstream, interacting with other jets, resulting in varied flow distribution patterns. Figure 4(b) displays the velocity vector field at the midplane of the channel, indicating a decline in the blowing ratio streamwise, enhancing the interaction between the jet and crossflow. Initially, with a high blowing ratio at the first jet, the jet impacts the bottom of the target surface perpendicularly, exerting a dominant impingement effect. Subsequently, with successive jets and the emergence of stagnation regions, deviation downstream occurs due to the crossflow influence. As the crossflow strengthens moving to end of impingement channel, the jets deviation intensifies. Additionally, the rearmost jets fail to impact the target directly. Therefore, the crossflow primarily influences the flow structure downstream of the target plate.

Table 3. Grid independence test for averaged Nusselt number of impinging jet array.

Grid system	Number of cells (Million)	Nu
coarser	0.67	55.04
coarse	1.1	60.89
normal	1.8	61.58
fine	3.4	61.60

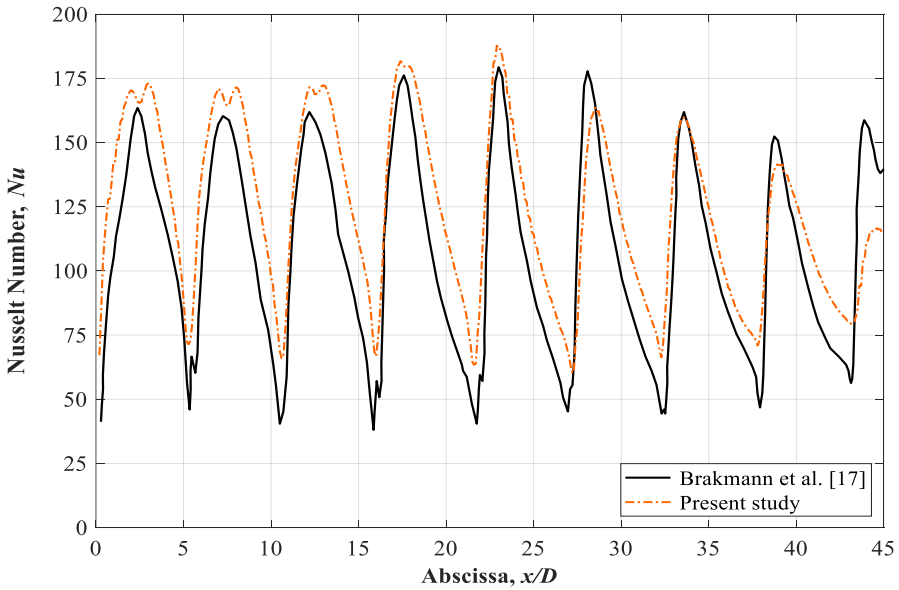

Fig. 3. Validation of the numerical procedure.

3.2. Heat transfer

Figure 5 illustrates the local Nusselt number over the curved target surface for the centered jet array with $P_j = 5$, $E_j = 0$, and $\theta = 0°$. According to the depicted figure, the distribution of the Nusselt number is closely linked with the flow pattern above the target surface. The findings indicate three behavioral regions in jet array impingement scenarios [7]. The jet strikes the target surface perpendicularly in the initial region, characterized by a lack of crossflow and absence of jet deviations. Here, the distribution of the Nusselt number resembles that of single-jet impingement, with values decreasing radially from the center of the jet. Figure 5 illustrates that the behavior of the first upstream jet aligns with this classical impingement behavior region. In the second behavioral region, the core of the jet begins to deflect due to crossflow, resulting in the relocation of the stagnation region downstream. Both flows interact with each other in this scenario. The jet flow and crossflow collaboration enhances the turbulence transport at the stagnation region above the curved target, as evident for the second jet streamwise in Fig. 5. Next jets encounter a gradual increase in crossflow, resulting in a diminishing penetration of the jet flow into the boundary layer, so they are named transitional behavior region. As the blowing ratio decreases further downstream, the jet flow is diminished, and the crossflow is improved; thus, the dominance of crossflow over heat transfer becomes evident. Due to the gradual accumulation of jet flow, the Nusselt number continues to rise within the third region, which is termed the crossflow-dominated region.

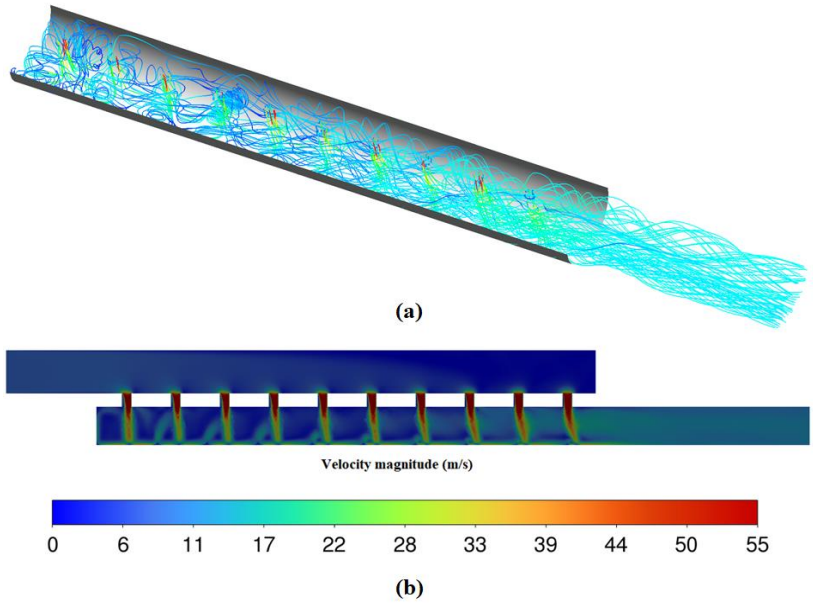

Fig. 4. The fluid flow characteristics of perpendicular ($\theta = 0°$) impingement array with $P_j = 5$ and no off-center distance ($E_j = 0$). (a) Isometric view, and (b) 2-D velocity contour at center plane of the impingement channel.

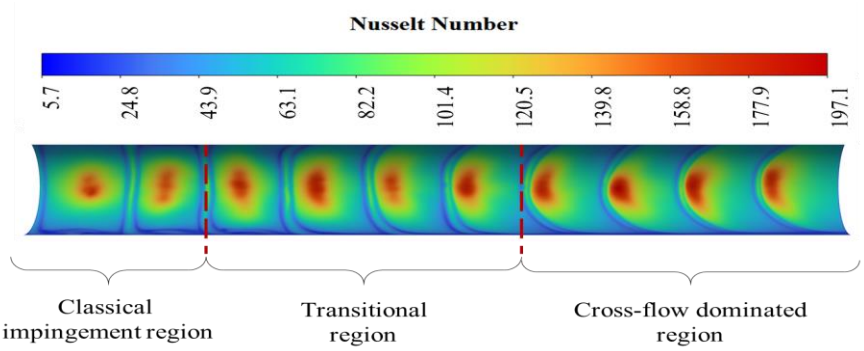

Fig. 5. Distribution of the jet array impingement Nusselt number on curved target for the geometry of $P_j = 5$, $\theta = 0°$, and $E_j = 0$.

3.3. Parametric study

In this study, numerical simulations are carried out to assess the impacts of design variables on the $\Delta\wp$, $\overline{Nu}$, and UI. The simulations cover the ranges of $2.5 \leq P_j \leq 10$, $0 \leq E_j \leq 6$, and $-45° \leq \theta \leq 45°$ for a constant mass flow rate.

3.3.1. Jet spacing (P_j)

Figure 6 demonstrates the effect of variations in jet spacing on average Nusselt number, heat transfer uniformity, and air pressure drop. The other design variables are held constant at $\theta = 0°$, and $E_j = 0$. According to this figure, the Nusselt number is directly related to jet spacing. Increasing jet spacing reduces the number of jets in the array, which leads to an increased velocity at each jet due to the constraint of a fixed total flow rate. Therefore, each of the jets strikes the target with higher momentum and turbulence energy. As a result, the local Nusselt number rises and enhances the average heat transfer over the target surface. Meanwhile, the increased local Nusselt number at the impingement points over the target deteriorates the uniformity index that is shown in the second figure. On the other hand, Fig. 6 shows a strongly rising trend between air pressure drop and jet spacing. With increased jet spacing comes an increased jet velocity, which elevates the pressure drop of jets.

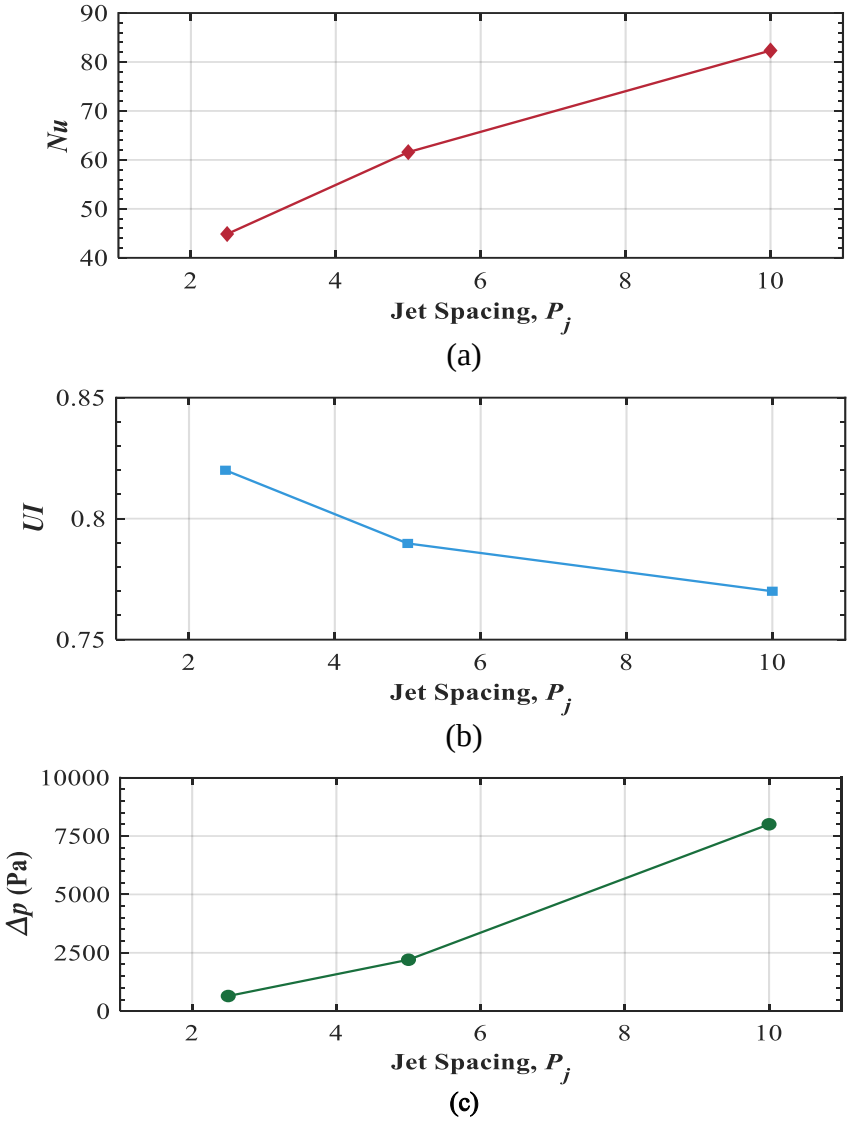

Fig. 6. Influence of jet spacing for $\theta = 0°$, and $E_j = 0$ on (a) $\overline{Nu}$, (b) UI, and (c) $\Delta\wp$.

3.3.2. The effect of jet inclination angle (θ)

Figure 7 represents the performance of an array with $P_j = 5$, and $E_j = 0$ under different jet inclination angles. According to the first figure, tilting the jet up to 15° both ways almost does not affect the heat transfer coefficient. However, for inclination angles larger than that, the Nusselt number reduces, especially at positive angles. In the case of inclined impingement, the jet must travel a longer distance to strike the target, yielding a larger momentum loss. Thus, the peak local Nusselt numbers decrease, which reduces the average Nusselt number over the surface. As for the uniformity index, the second figure shows that tilting the jet improves the uniformity due to the decreased local peaks of Nusselt number and increased areas under impingement of each jet. Moreover, as for the Fig. 7(c), the pressure drop is expected to grow at negative inclination angle owing to increased flow interactions between each jet and crossflow. Similarly, in positive angles, the larger the inclination angle, the smaller the imposed pressure drop.

3.3.3. Jet off-center distance (E_j)

The effect of asymmetry in jets' placement is shown in Fig. 8. Initially, increasing the off-center distance slightly reduces the average of the Nusselt number. Even though jet impaction is raised over one side of the curved target, a larger area of surface remains unaffected by the impingement. So, a decrease in the average Nusselt number is anticipated. However, beyond $E_j = 2$, the asymmetry leads to the formation of strong swirl flows near the target wall and increases the heat transfer coefficient, as shown by Fig. 8. In addition, based on the second figure, the effect of off-center distance on uniformity index is insignificant; but generally increasing the asymmetry more than $E_j = 2$, slightly increases the uniformity. Moreover, the effect of off-center distance on pressure drop is mildly descending. The reason can be justified by the fact that with increasing the off-center distance, the jet behavior on target tends to sliding rather than impaction and reduces the pressure drop. By changing the eccentricity from symmetric design, the average Nusselt number and uniformity index can improve to 16.5% and 1.85%, respectively. The pressure drop decrease up to 1.8%.

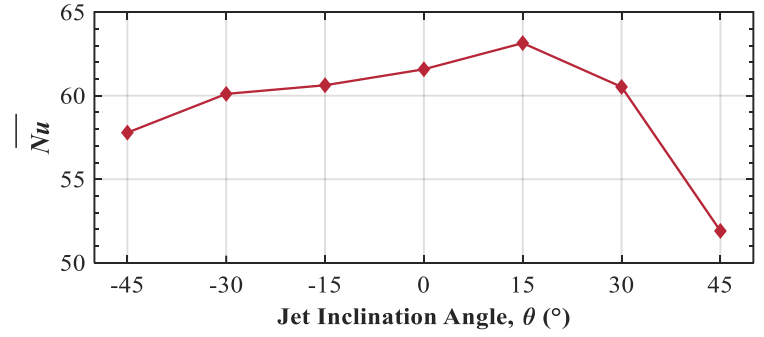

(a)

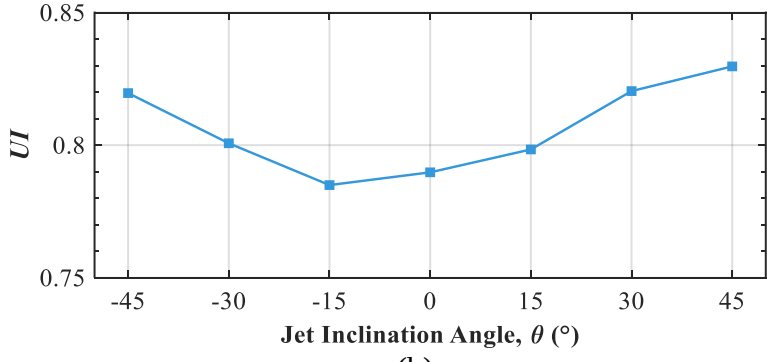

(b)

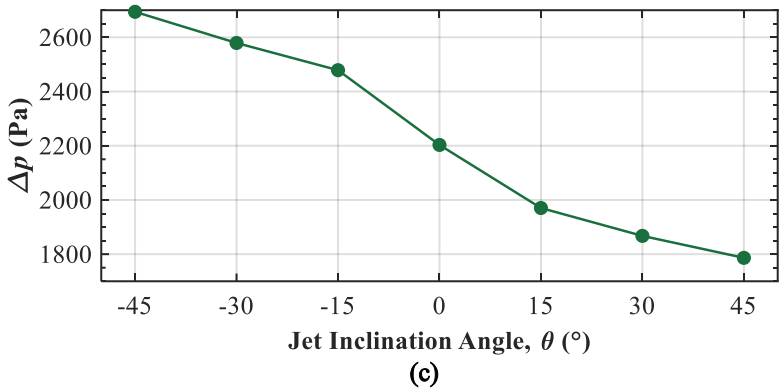

(c)

Fig. 7. Influence of jet inclination angle for $P_j = 5$, and $E_j = 0$ on (a) $\overline{Nu}$, (b) UI, and (c) Δp.

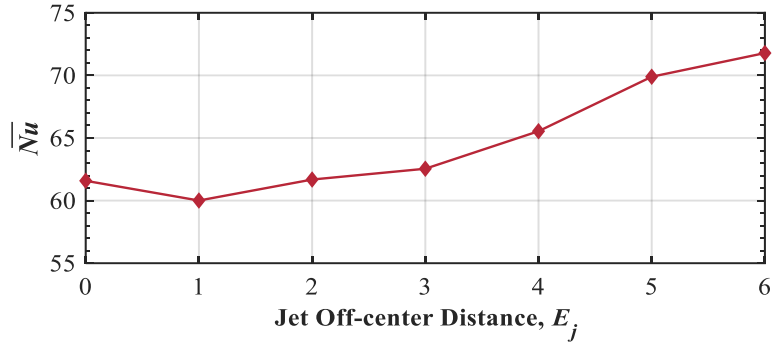

(a)

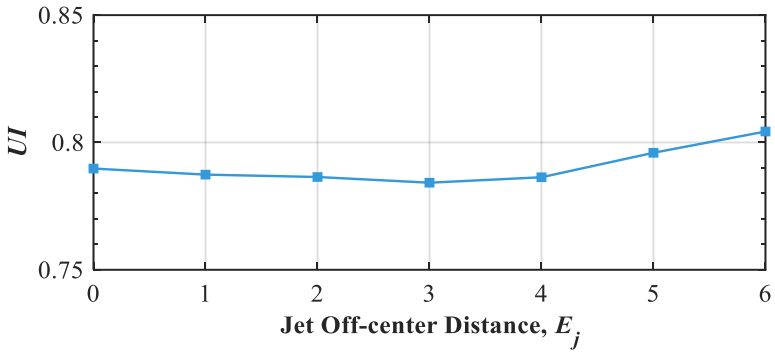

(b)

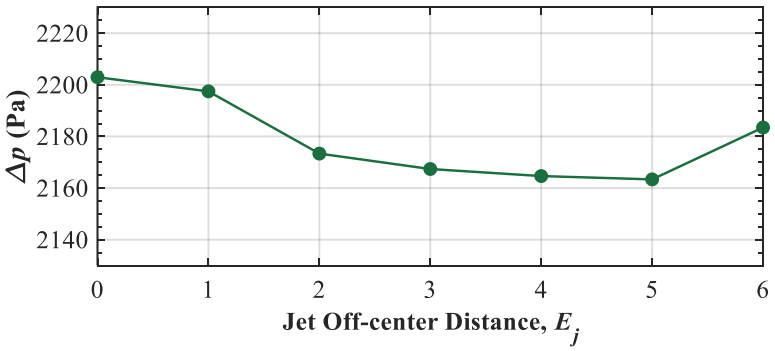

(c)

Fig. 8. Influence of jet off-center distance for $P_j = 5$, and $\theta = 0$ on (a) $\overline{Nu}$, (b) UI, and (c) Δp.

4. Conclusions

In the present research, we performed a parametric study in order to reveal the effect of different design variables on the performance of an impinging array of jets over semi-circular smooth channel. The geometrical parameters, including jet spacing (P_j), inclination angle (θ), and off-center distance (E_j), are investigated. The performance of cooling is evaluated by heat transfer uniformity index (UI), air pressure drop (Δp), and average Nusselt number ($\overline{Nu}$). The main results of this research are:

- Increasing the jet spacing leads to increased average Nusselt number and reduced uniformity. Also, pressure drop progressively increases with jet spacing.
- Tilting the jets in both positive and negative directions decrease the average Nusselt number except +15º; but improves the uniformity index with an exception in –15º. Air pressure drop reduces with increasing the angles from largest negative to largest positive.
- Adding asymmetry characteristics to the impingement array consistently reduces the pressure drop until the last eccentricity. At the same time, the uniformity index shows an almost independent behavior. The average Nusselt number decreases till $E_j = 2$, and rises beyond that value.
- Based on the findings, using the jet configuration with $P_j = 10$, θ=0, and $E_j = 0$ leads to a maximized average Nusselt number. Whereas, the case of $P_j = 5$, θ=45°, and $E_j = 0$ provides the most favorable uniformity index and pressure drop.

References

[1] Forster, M. and B. Weigand, Experimental and numerical investigation of jet impingement cooling onto a concave leading edge of a generic gas turbine blade. International Journal of Thermal Sciences, 2021. 164: p. 106862.

[2] Khan, M.S., et al., A comparison of oscillating sweeping jet and steady normal jet in cooling gas turbine leading edge: Numerical analysis. International Journal of Heat and Mass Transfer, 2023. 208: p. 124041.

[3] Chang, S.W. and J.L. Lee, Effect of grooved nozzle plate on aerothermal performance of rotating impingement-jet and pin-fin channel in axial-flow mode. International Journal of Heat and Mass Transfer, 2023. 217: p. 124664.

[4] Rao, Y., et al., Experimental and numerical studies on enhanced effusion cooling with shallowly dimpled film holes on double-wall structure surface. International Journal of Heat and Fluid Flow, 2023. 101: p. 109135.

[5] Zhou, J., et al., Numerical investigation on conjugate cooling performance of double swirl cooling at vane leading edge. International Journal of Thermal Sciences, 2023. 184: p. 107907.

[6] Luan, Y., Y. Rao, and H. Yan, Experimental and numerical study of swirl impingement cooling for turbine blade leading edge with internal ridged wall and film extraction holes. International Journal of Heat and Mass Transfer, 2023. 201: p. 123633.

[7] Jahromi, H.B. and F. Kowsary, A comprehensive parametric study and multi-objective optimization of turbulent jet array impingement for uniform cooling of gas turbine blades with minimized compression power. International Journal of Thermal Sciences, 2024. 201: p. 109035.

[8] Taghinia, J., M.M. Rahman, and T. Siikonen, CFD study of turbulent jet impingement on curved surface. Chinese Journal of Chemical Engineering, 2016. 24(5): p. 588-596.

[9] Zhou, Y., et al., Experimental study of curvature effects on jet impingement heat transfer on concave surfaces. Chinese Journal of Aeronautics, 2017. 30(2): p. 586-594.

[10] Poitras, G.J., et al., Aerodynamic and heat transfer analysis of a impinging jet on a concave surface. International Journal of Thermal Sciences, 2017. 114: p. 184-195.

[11] Yang, B., et al., Experimental and numerical investigation of heat transfer in an array of impingement jets on a concave surface. Applied Thermal Engineering, 2017. 127: p. 473-483.

[12] Wu, W., et al., Leading edge impingement cooling analysis with separators of a real gas turbine blade. Applied Thermal Engineering, 2022. 208: p. 118275.
[13] Tepe, A.Ü., Numerical investigation of a novel jet hole design for staggered array jet impingement cooling on a semicircular concave surface. International Journal of Thermal Sciences, 2021. 162: p. 106792.
[14] Qiu, D., et al., On heat transfer and flow characteristics of jets impinging onto a concave surface with varying jet arrangements. Journal of Thermal Analysis and Calorimetry, 2020. 141: p. 57-68.
[15] Akgül, V., B. Kurşuncu, and H. Kaya, Response surface methodology-based multi-objective grey relation optimization for impinging jet cooling with Al2O3/water nanofluid on a curved surface. Neural Computing and Applications, 2023. 35(19): p. 13999-14012.
[16] Hossain, M.A., et al., Experimental investigation of innovative cooling schemes on an additively manufactured engine scale turbine nozzle guide vane. Journal of Turbomachinery, 2021. 143(5): p. 051004.
[17] Brakmann, R., et al., Experimental and numerical heat transfer investigation of an impinging jet array on a target plate roughened by cubic micro pin fins. Journal of Turbomachinery, 2016. 138(11): p. 111010.

.